Advances in Modern Agriculture (2021) Volume 2 Issue 1
doi: 10.54517/ama.v2i1.2061

Asia Pacific Academy of Science Pte. Ltd.

ORIGINAL RESEARCH ARTICLE

Fluorescence tracer method for analysis of droplet deposition pattern characteristics of the sprays applied via unmanned aerial vehicle

Ruirui Zhang[1,2,3,4], Longlong Li[1,2,3,4], Yao Wen[1,2,3,4], Liping Chen[1,2,3,4,*], Qing Tang[1,2,3,4], Tongchuan Yi[1,2,3,4], Jiaxing Song[1,2,3,4]

[1] *Beijing Research Center of Intelligent Equipment for Agriculture, Beijing 100097, China*

[2] *National Research Center of Intelligent Equipment for Agriculture, Beijing 100097, China*

[3] *National Center for International Research on Agricultural Aerial Application Technology, Beijing 100097, China*

[4] *Beijing Engineering Laboratory for Beidou Navigation of Agricultural Machinery and Intelligent Measurement and Control, Beijing 100097, China*

*** Corresponding author:** Liping Chen, chenlp@nercita.cn

ABSTRACT

With the development of agricultural aviation technologies and their application in agricultural production, unmanned aerial vehicles (UAV) have been widely used to control pests and diseases of crops. The high-speed rotation of the rotor in the UAV produces a powerful downwash, affecting the distribution of pesticide droplets on the ground. Understanding the spatial distribution of these droplets on the ground is important to evaluate the application quality of the pesticides and plays an important role in improving the spray system in the UAV and optimizing its operating parameters. Current methods for measuring the droplet deposition distributions use a number of collectors placed regularly on the ground to receive the droplets and measure their sizes; it is difficult for them to effectively obtain the deposition of all droplets due to the downwash of the UAV. This paper presents a new method to resolve this problem by improving the accuracy and spatial continuity of pesticide droplet measurement applied by an unmanned helicopter. The flying parameters of a 3WQF-80-10 unmanned helicopter used to spray pesticides were obtained from the high-precision Beidou navigation system, and the RQT-C-3 fluorescent whitening tracer with a mass fraction of 1.0% was used as the proxy for the pesticides. Two droplet collection methods—one using continuous strip paper and the other using individual water-sensitive paper—were used to measure the droplet deposition distribution. We divided the experimental field into three areas, with Areas 1 and 2 spaced 3 m apart and Areas 2 and 3 spaced 1m apart. A metal bracket 8 m long and 0.5 m away from the ground was placed in each area. Prior to the experiment, a piece of paper tape was fixed to the surface of the bracket, and the water-sensitive paper cards were placed evenly in the area 0.5 m away from the paper tape. There was one piece of paper tape and 15 water-sensitive papers in each area, and a total of six spray tests were performed based on the pro-designed flight parameters. The combinations of flight speed and flight height were: 2 m/s and 3 m, 2 m/s and 6 m, 2 m/s and 9 m, 3 m/s and 3 m, 3 m/s and 6 m, and 4 m/s and 9 m. The paper tape was detected by fluorescence spectroscopy analysis, and the water-sensitive papers were scanned using image processing software to obtain droplet deposition coverage rates. The results showed that the distribution curves of the coverage rate obtained by the paper tape method coupled with the fluorescence spectrum tracer were consistent with those obtained from the images of the water-

ARTICLE INFO
Received: 3 April 2021 | Accepted: 2 May 2021| Available online: 10 May 2021

CITATION
Zhang R, Li L, Wen Y, et al. Fluorescence tracer method for analysis of droplet deposition pattern characteristics of the sprays applied via unmanned aerial vehicle. *Advances in Modern Agriculture* 2021; 2(1): 2061. doi: 10.54517/ama.v2i1.2061

sensitive paper method, with the R2 being 0.88–0.96. Because not all fine droplets fell on the water-sensitive papers due to the effect of the high-speed rotating rotor, the coverage rate curve measured by the continuous fluorescence method had multiple peaks, and the value of its coverage rate was higher than that measured by the water-sensitive paper method. When the unmanned helicopter flew at a speed of 2 m/s and a height of 3 m, the coverage ratio obtained from the continuous fluorescence method was up 16.92% compared to that sampled from the individual water-sensitive paper method, while when the flight speed was 4 m/s at a height of 9 m, the coverage ratio in the latter was 97.77% higher than in the former. In terms of the impacts of unmanned helicopter operating conditions on coverage rate, when the helicopter flew at 2 m/s and a height of 3 m, the coverage rate of the droplets obtained from the two methods was the highest, being 8.34% for the continuous fluorescence method and 7.14% for the individual paper method. As the flight height and speed increased, the spatial coverage rate of the droplets decreased. In summary, the high-speed rotor of the UAV generates a downwash, making the droplets of pesticides move in different directions and resulting in a large spatial difference in their deposition on the ground. Therefore, the continuous sampling method is more adequate to evaluate the spatial distribution of the droplets. This study has implications for the study of detecting the deposition of pesticides and other agrochemicals applied by UAVs.

Keywords: unmanned aerial vehicle; pesticide; droplet deposition distribution; spectral analysis; fluorescent tracer

1. Introduction

With the continuous application and development of agricultural aviation technology, plant protection drones have been widely used in the field of agricultural plant protection due to their high operational efficiency and flexibility flexibility[1–4]. In the process of spraying pesticides with drones, the drift of droplets will cause chemical waste and environmental pollution problems. Research on the operation quality and droplet deposition effects of drones is gradually increasing[5–7]. The main factors include spray system parameters (nozzle type, spray pressure, nozzle installation angle), meteorological parameters, flight parameters, rotor wind field, etc.[8–15]. Comprehensive analysis of factors affecting droplet deposition, optimization of spray systems, and flight parameters is the current research focus. In terms of the effect of spray droplet deposition, wind tunnel tests[16–18], simulations[19–22] and field tests are mainly used. Among them, field tests can directly obtain deposition data through actual spraying, so they are of great importance. For practical significance, many scholars have carried out related research. Qiu et al.[23] studied the influence of CD-10 UAV flying height and speed on the uniformity of wheat deposition and the interaction relationship between the two factors and constructed a corresponding relationship model. Qin et al.[24] explored the deposition and distribution of N-3 UAV spray droplets in the corn canopy in the middle and late stages of growth and screened out the spraying parameters suitable for high-stalk crop spraying. Chen et al.[25] measured the three-dimensional wind speed of the UAV rotor downwash wind field using a wireless wind speed sensor measurement system and concluded the deposition and distribution of spray droplets on the rice canopy in the UAV downwash wind field. Wang et al.[26] used the droplet deposition variation coefficient and root mean square error as indicators to compare the deposition distribution of four typical domestic plant protection UAV spray droplets in the wheat canopy. In terms of spray deposition effect detection, there are mainly tracer methods, water-sensitive paper methods, sensor detection methods, and so on. The tracer method can accurately measure the deposition amount using a fluorescence/ultraviolet-visible spectrophotometer[27], and is often used to quantify and compare the deposition or drift effects of droplets under different application methods or application parameters; the water-sensitive paper method can be used by scanning equipment and Image analysis software obtains droplet deposition density and coverage in real time and can also be used to estimate droplet spectral parameters[28]; With the development of electronic information and sensing technology, photoelectric-based detection methods emerge as the times require. Kesterson et al.[29] developed a droplet collection system based on a resistive sensing array that can accurately measure droplet deposition amount and droplet size. Most of the

above methods use discrete sampling methods, and adjacent sampling points are separated by a certain distance[30]. However, during the flight of the plant protection UAV, the rotor rotates at a high speed, the vortex line of the downwash airflow and the fuselage are distorted, the movement trajectory of the droplets is complex and changeable, and the continuous distribution of liquid deposition is difficult to grasp.

In this paper, the 3WQF-80-10 plant protection drone is used as the test model, and it is equipped with a high-precision Beidou navigation system to carry out field spray experiments. Using water-sensitive paper and the detection system for the deposition characteristics of aerial spraying droplets based on the spectral tracer method[31,32], the deposition results of spray droplets under different flight parameters were obtained simultaneously, and the 3WQF-80-10 type plant protection was analyzed. Droplet deposition distribution characteristics of UAV spraying. By comparing continuous and discrete sampling methods, the detection effect and applicability of the aerial spraying droplet deposition characteristics detection system for droplet deposition are evaluated in order to provide the system for the application of the system in plant protection UAV spraying. The application of quality inspection provides a theoretical basis.

2. Analysis of the movement and deposition law of spray droplets in aerial spraying

Aerial pesticide application uses aerial operations. During the operation, the interaction between the aircraft body and the ambient wind will produce a flow field vortex structure. Among them, the wake vortex of a fixed-wing aircraft is larger in scale and has a quasi-two-dimensional shape. The paired parallel wake vortices generated by the wing can be maintained for a long time. The complexity of the flow structure is low, and the spray droplets can be deposited smoothly on the ground. distributed; the UAV rotor rotates relatively fast. When the wingtip vortex forms and moves downward, its overall shape is destroyed by the other rotor after half a cycle. At the same time, the wingtip vortex structure is also affected by the airflow of the fuselage and tail rotor, eventually forming a complex unsteady flow[33], and the deposition distribution of spray droplets varies greatly within the space affected by the air flow field.

During the drone application process, the trajectory of mist droplets in unsteady flow is mainly analyzed through CFD simulation. The particle force differential equation (BBO equation) in the Lagrangian coordinate system is used to solve the force process of fog droplets in the air[34]. Solving the BBO equation is

$$m_p \frac{\mathrm{d}u_p}{\mathrm{d}t} = -V_p \frac{\partial p}{\partial x} + 3\pi\mu d_p f(u_i - u_p) + \frac{\rho_i V_p (\dot{u}_i - \dot{u}_p)}{2} + \frac{3}{2} d_p^2 \sqrt{\pi\mu\rho_i} \int_0^t \frac{\dot{u}_i - \dot{u}_p}{\sqrt{t-x}} \mathrm{d}x + m_p g \quad (1)$$

in the formula, $-V_p \frac{\partial p}{\partial x}$ is the pressure gradient term; $\frac{\rho_i V_p (\dot{u}_i - \dot{u}_p)}{2}$ is the additional mass force term; $\frac{3}{2} d_p^2 \sqrt{\pi\mu\rho_i} \int_0^t \frac{\dot{u}_i - \dot{u}_p}{\sqrt{t-x}}$ is the Basset force term; $3\pi\mu d_p f(u_i - u_p)$ is the aerodynamic resistance term of the discrete phase particles; the resistance correction coefficient $f = \frac{C_D Re_p}{24\rho_p}$, where C_D is the resistance coefficient, dimensionless; u_i is the continuous phase speed, m/s; u_p is the velocity of discrete phase particles, m/s; $\dot{u}_i$ is the acceleration of the continuous phase, m/s^2; $\dot{u}_p$ is the acceleration of the discrete phase particles, m/s^2; μ is the dynamic viscosity of the fluid, Pa·s; ρ_i is the density s of the fluid continuous phase, kg/m^3; ρ_p is the density of discrete phase particles, kg/m^3; d_p is the particle size of the particles, μm; m_p is the particle mass, mg; g is the gravity acceleration, m/s^2; $Re_p = \frac{\rho_i d_{p|u_i - u_p|}}{\mu}$ is the relative Reynolds number of the particles.

The analysis shows that in the complex flow field of the downwash of the rotor, the particle velocity at different spatial positions at the same time and at different times at the same spatial position is randomly pulsating, which is determined by the nature of turbulent flow, and the fluid velocity varies with the amount

of change that occurs in time and space, which is called space-time pulsation. It can be seen from the BBO equation that the additional mass force term, basset force term, and aerodynamic resistance term will directly affect the discrete phase particle motion velocity u_p, and the particle motion velocity is not only affected by its own characteristic parameters such as mass, density, diameter, etc., but also the airflow. Pulsation can also cause changes in droplet velocity.

Further use the fog drip particle power balance equation to gradually integrate the motion trajectory of the fog drip on the discrete time step and calculate and analyze the movement speed of the fog drip on the sporty trajectory.

$$\frac{\mathrm{d}x}{\mathrm{d}t} = u_p \tag{2}$$

The above equation shows that the change in particle motion velocity u_p in the discrete phase will cause the particle motion trajectory to change. The particle motion speed is not only affected by the characteristics of the droplet itself but also by the airflow pulsation. The particle velocity and the particle motion trajectory are combined to solve the equation, and further It can be seen from the derivation that in a complex flow field, the velocity u_p of discrete phase particles has a large amount of space-time pulsation, which in turn affects the velocity pulsation term of the discrete phase droplet in the equation and the motion trajectory obtained by its integral, and finally directly determines the droplet's settlement area and position. The downwash flow of the plant protection drone is an unsteady rotating flow field, and the airflow pulsation is complex and changeable, which makes it difficult to predict the droplet deposition area. The traditional discrete sampling droplet deposition measurement method (the droplet receiving device is arranged at intervals) is used. It is difficult to accurately present the complete information of the droplet deposition distribution on the ground. Especially in the study of the influence of the rotor downwash on the droplet deposition distribution, the key information about the effect of the air flow on the droplets at a specific location may be missed, which may interfere with the research results. In order to solve the above problems, this study adopted detection system for the deposition characteristics of aerial spraying droplets based on spectral tracer technology[31,32] to capture the continuous deposition distribution curve of droplets in the spraying area to obtain the spraying process of the drone. More abundant deposition distribution information is expected to guide the optimization of the plant protection UAV spray system and aerodynamic layout and improve the quality of droplet deposition.

3. Materials and methods

3.1. Test equipment and methods

3.1.1. Instrument and equipment

The flight platform adopts 3WQF-80-10 suspended smart plant protection drone Anyang Quanfeng Aviation Plant Protection Technology Co., Ltd., Henan). The main performance parameters are shown in **Table 1**. The speed and height of the test operation are adjusted according to the test group test requirements and record.

Table 1. Performance parameters of plant protection unmanned aerial vehicle.

Parameters	Value
Airframe length/m	2.92
Airframe width/m	0.6
Airframe height/m	0.75
Rotor diameter/m	1.8
Maximum load/kg	10
UAV weight/kg	35

Airborne spray system by the cabinet, pump, rod, pipe infusion, and two centrifugal sprinklers, spray rod 1.1 m wide, centrifugal nozzle perpendicular to the axis plane spacing installed on both ends of the spray rod, such as nozzle direction down the vertical analysis shows that in the complex rotor downwash flow field, particle velocity at the same time the different space position, and at different moments in the same space location, random pulsation occurs, which is determined by the nature of turbulence. The variation of fluid velocity with time and space is called space-time pulsation. It can be seen from the BBO equation that the additional mass force term, basset force term, and aerodynamic drag term all directly affect the motion velocity of discrete phase particles. The particles are on the ground, and the maximum flow rate of a single nozzle is 1.5 L/min. In order to accurately control the flight parameters, the BDST-R300-BG Beidou navigation and positioning system was used to obtain high-precision positioning data in real time, and the flight controller adjusted the flight attitude in real time through the positioning data so as to ensure that the plant protection UAV could spray in strict accordance with the design parameters of the experimental group. The positioning system consists of two parts: a reference station and a mobile station. The reference station is used to receive satellite signals to determine geographical location information and receive differential data, and the differential signals are transmitted to the mobile station using a high-power radio station. The mobile station is installed on the upper part of the fuselage of the UAV to be tested to record operating route trajectory, flight height, and flight speed operating condition parameters. The horizontal static difference accuracy of the system is ± (2.5 + 1 × 10^{-6}D) mm, and the vertical static difference accuracy is ± (5 + 1 × 10^{-6}D) mm. D refers to the radius diameter (mm) centered at the reference station. The horizontal positioning accuracy of real-time Kinematic (RTK) was ± (10 + 1 × 10^{-6}D) mm, and the vertical positioning accuracy of dual-frequency RTK was ± (20 + 1 × 10^{-6}D) mm. The meteorological monitoring system monitors and records the ambient wind speed, wind direction, temperature, and humidity parameters in real time during the test.

3.1.2. Experimental design

The experiment was conducted at the National Precision Agriculture Research Demonstration Base in Changping District, Beijing, on 12, 2018. The deposition distribution of droplets was obtained by the fluorescence tracer method and the water-sensitive paper method, respectively. The fluorescence tracer method used a continuous cloth pattern of fluorescent paper tape, and the water-sensitive paper method used a dispersive pattern. The droplet-collecting device is composed of an aluminum bracket, fluorescent paper tape, and water-sensitive paper. Test sample point arrangement is shown in **Figure 1**. On behalf of the eppo unmanned aerial vehicle (UAV) flight direction arrow direction, in a single experiment, a vertical line direction set up 3 droplets collection areas, numbers of 1, 2, and 3, respectively (sampling zone 1 and zone 2 at 3.0 m intervals, sampling zone 2 and zone 3 at 1.0 m intervals), collected in a horizontal layout with 1 set of aluminum brackets. The support is 8 m long and 0.5 m high from the ground. Before the test, the fluorescent paper tape (7 m long, 19.3 mm wide) was horizontally spread on the surface of the support and fixed with dovetail clips to prevent the paper tape from turning over during the test. Water-sensitive paper cards (76 mm × 26 mm, Syngenta, Switzerland) near the paper tape were evenly arranged with an equal spacing of 0.5 m, and 15 cards were arranged in each collection area. There were a total of 45 water-sensitive paper sample collection points in the experimental area. In order to facilitate the identification of samples, the water-sensitive paper and paper tape were marked by the method of test group plus collection area. For example, in test group 1, the water-sensitive paper and paper tape obtained in collection area 1 were represented as W1-1 and P1-1, respectively, and so on.

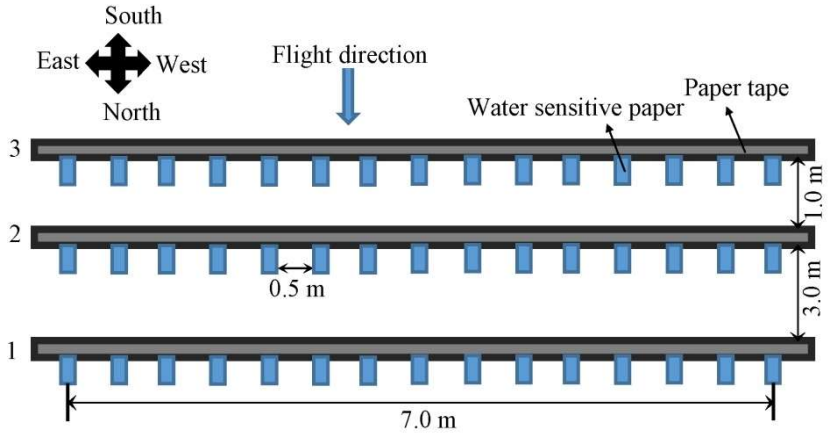

Figure 1. Schematic diagram of sampling arrangement in the test.
Note: 1, 2, and 3 represent collection area 1, collection area 2, and collection area 3, respectively.

The aqueous solution of fluorescent whitening agent RQT-C-3 (Ritter Company, Henan) with a mass fraction of 1.0% was used as the spray solution. In the test, the water-sensitive paper card and fluorescent paper tape were arranged to obtain the deposition distribution, coverage rate, and other key information about spray droplets. After the single spray test, the fog droplets on the surface of water-sensitive paper cards and paper tape were completely dried. Collect them according to the serial number, put them into the corresponding sealed bag one by one, and bring them back to the laboratory for testing.

3.1.3. Setting of flight operation parameters

Flight operation parameters are an important factor affecting the deposition and distribution of fog droplets. Previous studies have shown that different types of plant protection UAVs have different fuselage structures and different requirements on operation height, operation speed, and other parameters. In addition, there are specific requirements on operation parameters for the prevention and control of diseases and pests for different crops[35]. Many scholars have conducted test studies on droplet deposition distribution by flight parameters[36–38]. The flight altitude ranges from 1 to 9 m, and the flight speed ranges from 1 to 5 m/s. However, due to differences in application types, operating environments, application objects, and other factors, the optimal operating parameters vary. Through the survey, it was found that the current eppo UAV routine operation parameters for a speed of <8 m/s are apart from the crop canopy relative altitude of 1.5–5 m[39], Related studies have shown that unmanned aerial vehicles (UAV) under the condition of low-speed operation have good droplet coverage, especially the backspin air rotors, where the droplets are deposited directly on the positive and negative plant leaves[40]. However, the flight speed is too low, and the operation efficiency is difficult to guarantee. When the relative flight height is below 1 m, the operation safety of the UAV may be threatened. In consideration, combined with the unmanned aircraft manufacturers recommended job parameters, setting spray operation parameters, setting the speed to 3 levels (2 m/s for the low speed range, 3 m/s for the medium speed range, and more than 4 m/s for the high speed range), setting the setting the ground absolute altitude to 3, 6, 9 m, and 9 m height, The main consideration in this paper is that the design of the fluorescence tracer detection method for a kind of new detection method is still in the experimental stage. Conventional operation under the condition of detection effect is ideal, but the less the spray conditions or droplet deposition, the system can effectively detect, is unknown. For this design height 9 m homework, exploration under the condition of droplet deposition is less the applicability of the system. The combination of flight height and flight speed was used for six spraying tests (**Table 2**). Three samples of fluorescent paper tape and three groups of water-sensitive paper samples were obtained in each test. The flow rate of the single nozzle of the UAV spray system was set to 1.0 L/min.

Table 2. Flight and environmental parameters in the test.

Test No.	Mean flight speed /(m–s^{-1})	Mean flight height/m	Mean wind velocity/(m-s^{-1})	Wind direction	Mean temperature/°C	Mean relative humidity/%
1	2	3	0.5	The northwest	25.8	74.9
2	2	6	1.5	The northwest	25.5	76.3
3	2	9	1.0	The northwest	25.7	75.7
4	3	3	0.8	The northwest	25.9	73.3
5	3	6	1.0	The northwest	26.6	73.0
6	4	9	0.5	The northwest	26.4	73.0

3.2. Data acquisition and processing

3.2.1. Meteorological and flight operation parameters

During the test, an agricultural weather station (IWS-M400, Yujia Technology Co., Ltd..) was set up at a vertical distance of 2 m from the ground in the air. The changes in ambient wind speed, wind direction, temperature, and humidity during the test were monitored and recorded in real time through the meteorological monitoring system, and the average values of ambient wind speed, temperature, and humidity in each experimental group were obtained according to the statistical data. **Table 2** shows the UAV spraying operation parameters (average flying altitude and flying speed) obtained by the airborne Beidou positioning system and the corresponding meteorological parameters of each experimental group.

3.2.2. Fog drop deposition detection-water sensitive paper method

A TSN450 hand-held scanner (Tiencai Electronics (Shenzhen) Co., Ltd.., resolution: 1200 × 1200) was used to scan the water-sensitive paper samples one by one. The droplet deposition parameters on the surface of water-sensitive paper were obtained by image processing software ideas[41], and the droplet deposition coverage rate (%) of water-sensitive paper samples with different flight parameters was calculated and analyzed. The coverage rate of fog drops is the ratio of the dip-dyeing area of fog drops to the sampling area of water-sensitive test paper. The uniformity of droplet deposition among each collection point in the experiment was evaluated by the coefficient of variation (CV), which was calculated using the following formula:

$$CV=\frac{S}{\bar{X}}\times 100\% \tag{3}$$

$$S=\sqrt{\frac{\sum_{i=1}^{n}(X_i-\bar{X})^2}{n-1}} \tag{4}$$

In the formula, S is the standard deviation of the coverage rate of each group of collected samples, %; $\bar{X}$ is the average coverage rate, %; X_i is the droplet coverage rate of each collected sample, %; n is the number of collected samples. The smaller the CV value, the more uniform the droplet deposition distribution.

3.2.3. Droplet deposition detection—Fluorescence tracer method

The paper tape sample was scanned and processed by the airborne spray droplet deposition detection system[32], and the continuous distribution characteristic curve of the fluorescence medium spectrum on the surface of the whole paper tape was obtained. The system consists of a miniature spectrometer, stepper motor, ultraviolet light source, and photoelectric limiter. The fluorescence tracer RQT-C-3 on the surface of the paper tape generates molecular fluorescence under the excitation of an ultraviolet light source at 365 nm wavelength. The fluorescence light intensity information is converted into a digital signal through the light probe of the microspectrometer and finally transmitted and stored in the computer through a USB serial port. During the

acquisition process, the stepper motor drives the whole paper tape so that it is completely scanned. When the single piece of paper tape is collected, the photoelectric limiter responds back to the system and sends the instruction to stop the spectral data collection, and the stepper motor stops. The system acquisition time interval is set at 0.5 s, and the stepper motor speed is 120 r/min.

In 6 groups of experiments, a total of 18 paper tapes were obtained, and the number of sample points obtained by each paper tape was basically the same, and the number of spectral points of the paper tape was 102 or 103 groups. Equations (3) and (4) were used to calculate the coefficient of variation of droplet coverage in each experimental group.

4. Results and analysis

Figure 2 for the experimental group within the acquisition area 2 fluorescent tracer method and water sensitive paper method of droplets deposition rate distribution, the results show that the droplets are the main sedimentary in 1–5 m fabric sample interval, from the picture, we find that job parameters can affect the droplets deposition distribution, cause the droplets deposition distribution situation of the curve is different, when the speed of 2 m/s, When the working height is 3 m (**Figure 2A**), the waveform of the deposition curve changes significantly. With the increase in height (the working height is 6 m and 9 m, corresponding to tests 2 and 3, **Figure 2B** and **Figure 2C**), the distribution curve shows a gradual trend. The main reason is that the distance between the nozzle and the target increases with the increase in height. The fog droplets released from the nozzle disperse in the upper space of the target under the action of the downwash airflow field, resulting in relatively uniform deposition of the fog droplets settling on the target, but the coverage rate of the fog droplets is low.

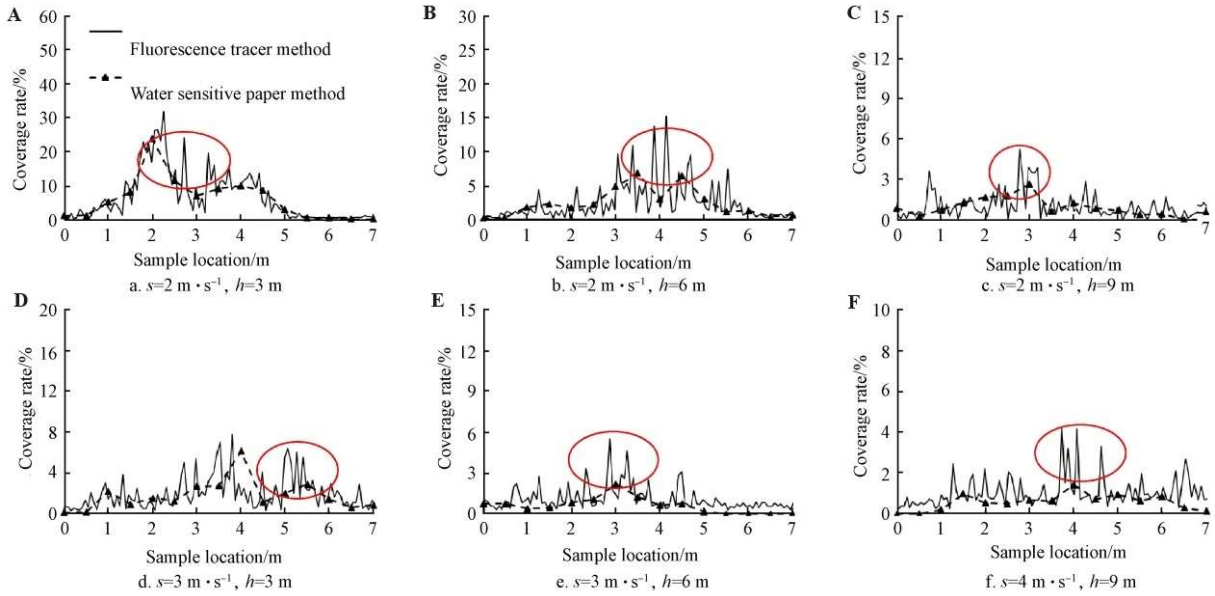

Figure 2. Deposition results of the tests in No.2 collecting area.
Note: *s* is flight speed, m·s^{-1}; *h* is flight height, m. The circle indicates the fluctuation of coverage rate obtained by the fluorescent tracer method.

For further analysis of the actual application performance of the fluorescence tracer method, the sedimentary curve is the most obvious change test 1 (**Figure 2A**) as the analysis object, and the water sensitivity paper method. Comparing the results of the droplet deposition distribution curves of the fluorescence tracer method and the water sensitive paper method, the droplet deposition distribution curve obtained overall uniformity, but the former coverage curve wave was higher than the latter. The highest

coverage rate was 31.92%, and the sample location was 2.25 m. The highest point of the coverage curve obtained by the water-sensitive paper method was 23.85% at 2.00 m. At the same time, compared with the dispersion sample method of the water-sensitive paper method, the coverage rate obtained by the fluorescence tracer method using the continuous measurement method showed multiple fluctuation peaks at different acquisition positions (marked by the solid circle in **Figure 2**), indicating that the effect of the downwash wind field of the unmanned helicopter resulted in large differences in the deposition space of fog droplets at each position in the vertical flight direction. In test 6 (**Figure 2F**), the flight speed and flight height were higher than those of the other five groups, the droplet coverage rate was low, the distribution curve obtained by the water-sensitive paper method was stable, and the droplet coverage curve detected by the fluorescence tracer method showed multiple obvious peak segments in the span direction. To further process the data from two methods, take the corresponding water-sensitive fluorescent tape, paper, and cloth sample location coverage data. With the water sensitivity of the paper measured, result fitting analysis, a single factor variance test (α = 0.05), the goodness of fit (R2), and the significance level as shown in **Table 3**, the analysis shows that the two methods for testing the droplet coverage results are in good correlation. The average goodness of fit of the six groups was 0.95, 0.92, 0.88, 0.92, 0.96, and 0.94, respectively. Under the conditions of experiments 1 to 5, there was no significant difference in droplet coverage obtained by the two methods (all P higher than 0.05). Only test 6 (flight speed of 4 m/s, flight altitude of 9 m) (P = 0.02) indicates that the detection method based on the fluorescence tracer can characterize the droplet deposition coverage parameters under conventional operation conditions of plant protection UAVs.

Table 3. Analysis of droplet coverage rate obtained by water sensitive paper method and fluorescent tracer method.

Item	**Test 1**			**Test 2**			**Test 3**			**Test 4**			**Test 5**			**Test 6**		
	1–1	**1–2**	**1–3**	**2–1**	**2–2**	**2–3**	**3–1**	**3–2**	**3–3**	**4–1**	**4–2**	**4–3**	**5–1**	**5–2**	**5–3**	**6–1**	**6–2**	**6–3**
R^2	0.98	0.92	0.96	0.94	0.92	0.91	0.91	0.89	0.84	0.89	0.92	0.96	0.94	0.95	0.98	0.97	0.96	0.89
P	0.91	0.75	0.74	0.60	0.56	0.92	0.27	0.73	0.79	0.56	0.41	0.24	0.24	0.77	0.97	0.12	0.08	0.02
RMSE	1.99	2.49	2.22	0.89	1.02	0.69	0.52	0.47	0.24	0.68	0.81	1.60	0.39	0.32	0.47	0.37	0.27	0.48

Table 4 shows two kinds of test methods for the droplet deposition and distribution of measured results. As can be seen from the table, the fluorescence tracer method to calculate the average droplet cover was higher than the water-sensitive paper method. The main reason is that the water-sensitive paper method uses the sample from the spreading way, plant protection, an unmanned aerial vehicle (UAV) rotor vortex causes droplets disorderly movement, and settlement of droplets are parts of the downwash flow under the action of concentrated water-sensitive paper location, not cloth. The peak shown in **Figure 2** appears. When the flying speed and flying altitude of the UAV are 3 m/s and 3 m, respectively, the change rate of the fluorescence tracer method is the lowest compared with the water-sensitive paper method, which is 8.71%. When the flight speed is 2 m/s, the average coverage change of the UAV is 47.58% at the flight height of 9 m, which is significantly higher than that at the flight heights of 3 and 6 m. When the flight height was constant (test groups 2 and 5, test groups 3 and 6), the change rate of droplet coverage was positively correlated with the flight speed. The higher the flight speed, the higher the change in droplet coverage. When the flight speed was 4 m/s and the altitude was 9 m, the change rate of the fluorescence tracer method relative to the water-sensitive paper method could reach 97.77%. In conclusion, the increasing eppo unmanned aerial vehicle (UAV) flight velocity and altitude, the water sensitive paper method, and the deposition of discrete sampling methods with the fluorescence tracer method of continuous sampling result in deviation. The more likely reason is that the increase in speed and altitude can contain high-tiny droplets of wingtip vortex movement down stress orientation deposit, and the and the settlement of droplets to the location of water sensitive paper to collect

leads to a deviation increase. At present, plant protection under the under the unmanned aerial vehicle (UAV) with low volume or low volume spray technology, tiny droplets in the rotor downwash under the action of the wind field, the ground of droplets deposition space difference is big; therefore, in the plant protection under the unmanned aerial vehicle (UAV) wash the wind field distribution on the droplet's deposition impact study, continuous sampling should be done in order to get more space to droplet deposition distribution in detail. In terms of the variation coefficient within the sampling interval, the average variation rate of fluorescent paper tape relative to water-sensitive paper ranges from 1.67% to 29.71%. Because the fluorescence tracer method adopts continuous sampling, the coverage distribution curve has obvious multiple peaks in the non-water-sensitive paper cloth sample position, so the coverage range of fog drops in the sampling range is higher than the test results of the water-sensitive paper method.

Table 4. Droplet deposition measured by water sensitive paper method and fluorescent tracer method.

Test No.	Collection area	Droplet coverage rate/%			Coefficient of variation of sampling/%			Range of coverage rate/%		
		Fluorescence tracer method	Water sensitive paper method	Rate of change	Fluorescence tracer method	Water sensitive paper method	Rate of change	Fluorescence tracer method	Water sensitive paper method	Difference
1	1	10.13	8.77	15.51	119.16	120.48	1.09	45.62	29.98	15.64
	2	7.02	6.10	15.08	104.57	104.38	0.18	31.62	23.63	8.01
	3	7.86	6.54	20.18	101.56	105.51	3.74	38.45	21.67	16.78
	Average	8.34	7.14	16.92	108.43	110.12	1.67	38.56	25.09	13.48
2	1	2.63	2.43	8.23	92.62	84.72	9.32	9.65	6.16	3.49
	2	2.41	2.35	2.55	118.03	89.98	31.17	15.10	6.64	8.46
	3	2.34	1.83	27.87	101.97	90.68	12.45	10.86	5.35	5.51
	Average	2.46	2.20	12.88	104.21	88.46	17.65	11.87	6.05	5.82
3	1	1.27	0.86	47.67	87.25	68.93	26.58	5.99	2.08	3.91
	2	1.07	0.94	13.83	92.20	75.64	21.89	5.21	2.59	2.62
	3	1.16	0.64	81.25	97.46	69.28	40.67	8.07	1.56	6.51
	Average	1.17	0.81	47.58	92.30	71.28	29.71	6.42	2.08	4.35
4	1	2.06	1.90	8.42	71.11	71.92	1.12	6.35	5.12	1.23
	2	2.06	1.82	13.19	78.95	82.16	3.91	7.44	6.03	1.41
	3	2.32	2.43	4.53	86.42	105.57	18.14	9.57	9.24	0.33
	Average	2.15	2.05	8.71	78.83	86.55	7.72	7.79	6.80	0.99
5	1	1.42	0.92	54.34	70.55	78.18	9.76	5.57	2.49	3.08
	2	1.14	0.63	80.95	78.36	95.37	17.84	5.22	2.20	3.02
	3	1.29	0.82	57.32	88.35	148.94	40.68	7.07	4.82	2.25
	Average	1.28	0.79	64.20	79.09	107.50	22.76	5.95	3.17	2.78
6	1	1.17	0.65	80.00	69.50	86.10	19.28	4.64	1.99	2.65
	2	1.07	0.58	84.48	69.23	68.41	1.20	4.00	1.43	2.57
	3	1.19	0.52	128.84	66.40	78.00	14.87	3.80	1.25	2.55
	Average	1.14	0.58	97.77	68.38	77.50	11.78	4.15	1.56	2.59

Note: Rate of change represents the absolute value changed rate relative to water sensitive paper method.

Figure 3 shows the droplet deposition coverage rate of the plant protection UAV under different working

conditions. The results show that the droplet deposition coverage rate is the highest under the working conditions of flying speed of 2 m/s and flying altitude of 3 m, and the results obtained by the fluorescence tracer method and the water-sensitive paper method are 8.34% and 7.14%, respectively. With the increase in flying altitude, the coverage rate of droplet deposition gradually decreases. When the flying speed is 2 m/s, the coverage rate of 6 m flying altitude decreases by 52.4% and 63.18% compared with 3 m flying altitude under two measurement methods. When the flight altitude is 6 m, the droplet coverage rate at 3 m/s is 47.97% and 64.10% lower than that at 2 m/s, respectively, which indicates that increasing the flight speed will reduce the number of droplets effectively deposited on the target surface. As the fog drops under the plant protection UAV are greatly influenced by the turbulent wind field caused by the wing and the external wind field, with the increase of the aircraft's operating speed and flying altitude, the flow field of the rotor's downspin airflow in the direction perpendicular to the ground decreases, and the energy content of the wing tip vortex increases, which drives the fog drops to curl up, resulting in an increase in fog drop drift and a corresponding decrease in fog drop deposition in the target area. In addition, increasing the flying height correspondingly increases the movement distance of droplets in the air, and it is easy to sink to the non-target application area under the action of environmental wind. For high-stalk crops such as sugarcane and corn, the job safety and droplet deposition quality should be considered comprehensively, and the height of the UAV relative to the crop canopy should not be too low.

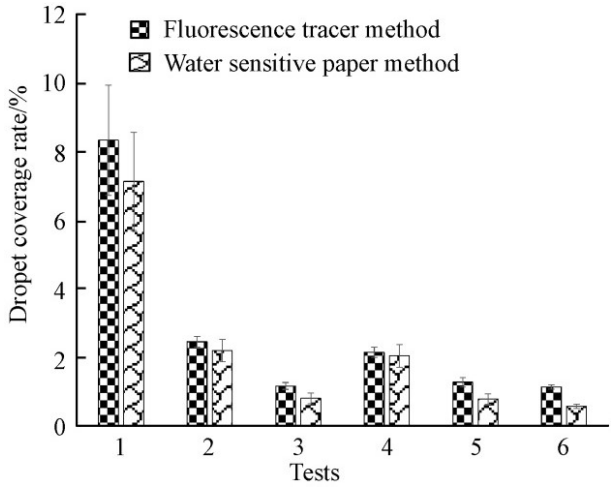

Figure 3. Droplet coverage rates under different working conditions.

5. Conclusion

In this paper, the flight parameters of the plant protection UAV are obtained by a high-precision Beidou navigation system, and the spray test of the 3WQF-80-10 plant protection UAV under different flight parameters is carried out by using a 1.0% RQT-C-3 fluorescent whitening agent water solution instead of pesticide. Two droplet collection methods, namely continuous cloth sampling with long paper tape and scattered sampling with water-sensitive paper, are adopted, and the droplet deposition coverage is obtained by the fluorescence tracing method and image processing with water-sensitive paper. The droplet deposition distribution characteristics of the two sampling methods are compared and analyzed. The following conclusions are drawn:

- The distribution curves of droplet deposition coverage obtained by the fluorescence tracing method and the water-sensitive paper method tend to be consistent, with a root mean square error of 0.24%–2.49%. The results of droplet coverage obtained by the two detection methods have a good correlation, and the

goodness of fit (R^2) ranges from 0.88 to 0.96. Only under the condition of experimental group 6 (flying speed 4 m/s, flying height 9 m), the results of droplet coverage obtained by the two methods are as follows.

- Compared with the water-sensitive paper sample separation method, the coverage curve obtained by continuous sample distribution based on fluorescence tracing has several peaks, and the average coverage of droplets in the latter is higher than that in the former. When the flying speed of the plant protection UAV is 4 m/s and the relative target height is 9 m, the coverage obtained by the fluorescence tracing method is increased by 97.77% compared with that of the water-sensitive paper sample separation method, and the deposition results obtained by the sample separation method are difficult to effectively characterize the overall droplet deposition distribution in the spraying spray, mainly because the wingtip vortex generated by the plant protection UAV flight drives the droplets to be non-existent.
- Under the experimental conditions in this paper, droplet deposition is affected by the flying speed and relative target altitude. When the flying speed is 2 m/s, the coverage rate at 6 m flying relative altitude is 52.40% lower than that at 3 m; when the relative altitude is 6 m, the droplet coverage rate at 3 m/s is 47.97% lower than that at 2 m/s.

To sum up, the UAV for plant protection works in the air, and the downwash airflow generated by the high-speed rotating rotor drives the droplets to deposit non-directionally, which leads to the sharp fluctuation of droplet deposition density in small-scale space. Therefore, when the UAV for plant protection detects the ground deposition quality or studies the influence of the downwash wind field on droplet deposition distribution, continuous sample distribution should be adopted so as to evaluate the overall droplet deposition distribution more concretely and comprehensively.

Conflict of interest

The authors declare no conflict of interest.

References

1. Zhou Z, Zang Y, Luo X, et al. Technology innovation development strategy on agricultural aviation industry for plant protection in China. *Transactions of the Chinese Society of Agricultural Engineering (Transactions of the CSAE)* 2013; 29(24): 1–10.
2. Zhang D, Lan Y, Chen L, et al. Current status and future trends of agricultural aerial spraying technology in China. *Transactions of the Chinese Society for Agricultural Machinery* 2014; 45(10): 53–59. doi: 10.6041/j.issn.1000-1298.2014.10.009
3. Faiçal BS, Freitas H, Gomes PH, et al. An adaptive approach for UAV-based pesticide spraying in dynamic environments. *Computers and Electronics in Agriculture* 2017; 138: 210–223. doi: 10.1016/j.compag.2017.04.011
4. Li L, Liu Y, He X, et al. Assessment of spray deposition and losses in the apple orchard from agricultural unmanned aerial vehicle in China. *2018 ASABE Annual International Meeting* 2018; 1800504. doi:10.13031/aim.201800504
5. Huang Y, Hoffmann WC, Lan Y, et al. Development of a spray system for an unmanned aerial vehicle platform. *Applied Engineering in Agriculture* 2009; 25(6): 803–809. doi: 10.13031/2013.29229
6. He Y, Wu J, Fang H, et al. Research on deposition effect of droplets based on plant protection unmanned aerial vehicle: A review. *Journal of Zhejiang University (Agriculture and Life Sciences)* 2018; 44(4): 392–398. doi: 10.3785/j.issn.1008-9209.2018.07.020
7. Liao J, Zang Y, Zhou Z, et al. Quality evaluation method and optimization of operating parameters in crop aerial spraying technology. *Transactions of the Chinese Society of Agricultural Engineering (Transactions of the CSAE)* 2015; 31(Supp.2): 38–46.
8. Tang Q, Zhang R, Chen L, et al. Droplets movement and deposition of an eight–rotor agricultural UAV in downwash flow field. *International Journal of Agricultural and Biological Engineering* 2017; 10(3): 47–56. doi: 10.3965/j.ijabe.20171003.3075
9. Zhou Q, Xue X, Qin W, et al. Optimization and test for structural parameters of UAV spraying rotary cup atomizer. *International Journal of Agricultural and Biological Engineering* 2017; 10(3): 78–86. doi: 10.3965/j.ijabe.20171003.3119

10. Zhang R, Zhang Z, Xu G, et al. Effect of spray adjuvant types and concentration on nozzle atomization. *Transactions of the Chinese Society of Agricultural Engineering (Transactions of the CSAE)* 2018; 34(20): 36–43.
11. Zhang J, He X, Song J, et al. Influence of spraying parameters of unmanned aircraft on droplets deposition. *Transactions of the Chinese Society for Agricultural Machinery* 2012; 43(12): 94–96. doi: 10.6041/j.issn.1000-1298.2012.12.017
12. Li J, Lan Y, Shi Y. Research progress on airflow characteristics and field pesticide application system of rotary-wing UAV. *Transactions of the Chinese Society of Agricultural Engineering (Transactions of the CSAE)* 2018; 34(12): 104–118. doi: 10.11975/j.issn.1002-6819.2018.12.013
13. Zhang P, Li Q, Yi S L, et al. Evaluation of spraying effect using small unmanned aerial vehicle (UAV) in citrus orchard. *Journal of Fruit Science* 2016; 33(1): 34–42.
14. Yang Z, Ge L, Qi L, et al. Influence of UAV rotor down-wash airflow on spray width. *Transactions of the Chinese Society for Agricultural Machinery* 2018; 49(1): 116–122. doi: 10.6041/j.issn.1000-1298.2018.01.014
15. Wen S, Han J, Lan Y, et al. Influence of wing tip vortex on drift of single rotor plant protection unmanned aerial vehicle. *Transactions of the Chinese Society for Agricultural Machinery* 2018; 49(8): 127–137. doi: 10.6041/j.issn.1000-1298.2018.08.015
16. Nuyttens D, Taylor WA, De Schampheleire M, et al. Influence of nozzle type and size on drift potential by means of different wind tunnel evaluation methods. *Biosystems Engineering* 2009; 103(3): 271–280. doi: 10.1016/j.biosystemseng.2009.04.001
17. Ru Y, Zhu C, Bao R. Spray drift model of droplets and analysis of influencing factors based on wind tunnel. *Transactions of the Chinese Society for Agricultural Machinery* 2014; 45(10): 66–72. doi: 10.6041/j.issn.1000-1298.2014.10.011
18. Zhang R, Li L, Fu W, et al. Spraying atomization performance by pulse width modulated variable and droplet deposition characteristics in wind tunnel. *Transactions of the Chinese Society of Agricultural Engineering (Transactions of the CSAE)* 2019; 35(3): 42–51. doi: 10.11975/j.issn.1002-6819.2019.03.006
19. Delele MA, Jaeken P, Debaer C, et al. CFD prototyping of an air-assisted orchard sprayer aimed at drift reduction. *Computers and Electronics in Agriculture* 2007; 55(1): 16–27. doi: 10.1016/j.compag.2006.11.002
20. Zheng Y, Yang S, Zhao C, et al. Modelling operation parameters of UAV on spray effects at different growth stages of corns. *International Journal of Agricultural and Biological Engineering* 2017; 10(3): 57–66. doi: 10.3965/j.ijabe.20171003.2578
21. Duga AT, Delele MA, Ruysen K, et al. Development and validation of a 3D CFD model of drift and its application to air-assisted orchard sprayers. *Biosystems Engineering* 2017; 154: 62–75. doi: 10.1016/j.biosystemseng.2016.10.010
22. Zhang B, Tang Q, Chen L ping, et al. Numerical simulation of spray drift and deposition from a crop spraying aircraft using a CFD approach. *Biosystems Engineering* 2018; 166: 184–199. doi: 10.1016/j.biosystemseng.2017.11.017
23. Qiu B, Wang L, Cai D, et al. Effects of flight altitude and speed of unmanned helicopter on spray deposition uniform. *Transactions of the Chinese Society of Agricultural Engineering (Transactions of the CSAE)* 2013; 29(24): 25–32. doi: 10.3969/j.issn.1002-6819.2013.24.004
24. Qin W, Xue X, Zhou L, et al. Effects of spraying parameters of unmanned aerial vehicle on droplets deposition distribution of maize canopies. *Transactions of the Chinese Society of Agricultural Engineering (Transactions of the CSAE)* 2014; 30(5): 50–56. doi: 10.3969/j.issn.1002-6819.2014.05.007
25. Chen S, Lan Y, Li J, et al. Effect of wind field below unmanned helicopter on droplet deposition distribution of aerial spraying. *International Journal of Agricultural and Biological Engineering* 2017; 10(3): 67–77. doi: 10.3965/j.ijabe.20171003.3078
26. Wang C, Song J, He X, et al. Effect of flight parameters on distribution characteristics of pesticide spraying droplets deposition of plant-protection unmanned aerial vehicle. *Transactions of the Chinese Society of Agricultural Engineering (Transactions of the CSAE)* 2017; 33(23): 109–116. doi: 10.11975/j.issn.1002-6819.2017.23.014
27. Torrent X, Garcerá C, Moltó E, et al. Comparison between standard and drift reducing nozzles for pesticide application in citrus: Part I. Effects on wind tunnel and field spray drift. *Crop Protection* 2017; 96: 130–143. doi: 10.1016/j.cropro.2017.02.001
28. Sharda A, Karkee M, Zhang Q, et al. Effect of emitter type and mounting configuration on spray coverage for solid set canopy delivery system. *Computers and Electronics in Agriculture* 2015; 112: 184–192. doi: 10.1016/j.compag.2014.07.012
29. Kesterson M, Luck J, Sama M. Development and preliminary evaluation of a spray deposition sensing system for improving pesticide application. *Sensors* 2015; 15(12): 31965–31972. doi: 10.3390/s151229898
30. Bae Y, Koo YM. Flight attitudes and spray patterns of a roll-balanced agricultural unmanned helicopter. *Applied Engineering in Agriculture* 2013; 29(5): 675–682. doi: 10.13031/aea.29.10059
31. Zhang R, Wen Y, Yi T, et al. Development and application of aerial spray droplets deposition performance

measurement system based on spectral analysis technology. *Transactions of the Chinese Society of Agricultural Engineering (Transactions of the CSAE)* 2017; 33(24): 80–87. doi: 10.11975/j.issn.1002-6819.2017.24.011
32. Wen Y, Zhang R, Chen L, et al. A new spray deposition pattern measurement system based on spectral analysis of a fluorescent tracer. *Computers and Electronics in Agriculture* 2019; 160: 14–22. doi: 10.1016/j.compag.2019.03.008
33. Seddon J, Newman S. *Basic Helicopter Aerodynamics*, 3rd ed. Aerodynamics & Flight Mechanics Group; 2011. doi: 10.2514/4.868610
34. Hjelmfelt AT, Mockros LF. Motion of discrete particles in a turbulent fluid. *Applied Scientific Research* 1966; 16(1): 149–161. doi: 10.1007/bf00384062
35. Giles D, Billing R. Deployment and performance of a UAV for crop spraying. *Chemical Engineering Transactions* 2015; 44: 307–312. doi: 10.3303/CET1544052
36. Qin WC, Qiu BJ, Xue XY, et al. Droplet deposition and control effect of insecticides sprayed with an unmanned aerial vehicle against plant hoppers. *Crop Protection* 2016; 85: 79–88. doi: 10.1016/j.cropro.2016.03.018
37. Wang J, Luo B, Huo Y, et al. Influence of adjuvant on large-scale plant protection UAV spray characteristics. *Journal of Drainage and Irrigation Machinery Engineering* 2019; 37(12): 1044–1049.
38. Tang Y, Hou CJ, Luo SM, et al. Effects of operation height and tree shape on droplet deposition in citrus trees using an unmanned aerial vehicle. *Computers and Electronics in Agriculture* 2018; 148: 1–7. doi: 10.1016/j.compag.2018.02.026
39. He X. Brief analysis on the research, development and application of plant protection UAV in China. *Pesticide Science and Administration* 2018; 39(9): 20–27.
40. He X. Spray system and application technology of plant protection UAV in China. *Agricultural Engineering Technology* 2018; 38(9): 33–38. doi:10.16815/j.cnki.11-5436/s.2018.09.006
41. Xu G, Chen L, Zhang R. An image processing system for evaluation of aerial application quality. In: Proceedings of the 2016 International Conference on Intelligent Information Processing; 23–25 December 2016; Wuhan, China.